

Minimizing the fissile inventory of the molten salt fast reactor

E. Merle-Lucotte, D. Heuer, M. Allibert, X. Doligez, V. Ghetta

► **To cite this version:**

E. Merle-Lucotte, D. Heuer, M. Allibert, X. Doligez, V. Ghetta. Minimizing the fissile inventory of the molten salt fast reactor. Advances in Nuclear Fuel Management IV (ANFM IV), Apr 2009, Hilton Head Island, United States. in2p3-00385378

HAL Id: in2p3-00385378

<http://hal.in2p3.fr/in2p3-00385378>

Submitted on 9 Jun 2009

HAL is a multi-disciplinary open access archive for the deposit and dissemination of scientific research documents, whether they are published or not. The documents may come from teaching and research institutions in France or abroad, or from public or private research centers.

L'archive ouverte pluridisciplinaire **HAL**, est destinée au dépôt et à la diffusion de documents scientifiques de niveau recherche, publiés ou non, émanant des établissements d'enseignement et de recherche français ou étrangers, des laboratoires publics ou privés.

MINIMIZING THE FISSILE INVENTORY OF THE MOLTEN SALT FAST REACTOR

E. Merle-Lucotte, D. Heuer, M. Allibert, X. Doligez, V. Ghetta

LPSC-IN2P3-CNRS / UJF / Grenoble INP

Address: LPSC, 53 avenue des Martyrs, 38026 Grenoble Cedex - France

merle@lpsc.in2p3.fr

Keywords: Molten Salt Reactor, Thorium fuel cycle, fast neutron spectrum

ABSTRACT

Molten salt reactors in the configurations presented here, called Molten Salt Fast Reactors (MSFR), have been selected for further studies by the Generation IV International Forum. These reactors may be operated in simplified and safe conditions in the Th/²³³U fuel cycle with fluoride salts. We present here the concept, before focusing on a possible optimization in term of minimization of the initial fissile inventory. Our studies demonstrate that an inventory of ²³³U lower than 4 metric tons per GWe may be easily reached, and bring to light the limitations of the concept due to the irradiation damages to the structural materials and to the capacities of the heat exchangers. We conclude that these two issues will have to be studied in depth to allow a realistic evaluation of the global possibilities of such a reactor.

1. INTRODUCTION

Starting from the Oak-Ridge Molten Salt Breeder Reactor project¹, we have performed some parametric studies^{2,3,4,5,6} correlating the core arrangement, the reprocessing performances, and the salt composition, in terms of safety coefficients, reprocessing requirements, and breeding capabilities. In the frame of this major re-evaluation of the molten salt reactor (MSR), we have thus developed a new concept that we called the Thorium Molten Salt Reactor (TMSR), which is particularly well suited to fulfil the criteria chosen by the Generation IV International Forum.

This reactor may be operated in simplified and safe conditions in the Th/²³³U fuel cycle with fluoride salts. Its main advantages, due to the liquid fuel and coolant and to the thorium cycle, are the following: the amounts of fissile and fertile matter can be adjusted without unloading the core, avoiding any initial reactivity reserve; the Fission Products which poison the core can be quickly extracted; nuclear waste production is minimized; very high temperatures may be reached without requiring high pressure in the core.

Amongst all TMSR configurations, our recent studies have singled out the configurations with no moderator in the core: they are simple and very promising, the moderation ratio depending only on the salt composition. Such a reactor presents many

intrinsic advantages, in addition to avoiding the deterioration of the moderator while ensuring excellent safety characteristics. In previous articles we presented this reactor under the name “non-moderated Thorium Molten Salt Reactor” or TMSR-NM. With a fuel salt content low in light elements a fast neutron spectrum is obtained. This concept, now called Molten Salt Fast Reactor or MSFR, has been selected for further studies by the Generation IV International Forum.

For the most promising versions of the MSFR previously presented^{7,8}, the initial fissile load was quite large, around 5 to 6 metric tons of ²³³U. This concept is reliable and robust enough to allow further optimizations, among which a minimization of the fissile inventory. In this paper, we will review the MSFR concept, before focusing on the minimization of the initial fissile inventory necessary to start the reactor, the limitations being due to the irradiation damages to the structural materials and to the capacities of the heat exchangers.

Our neutronic results rely on numerical simulations making use of the MCNP neutron transport code⁹ coupled with an in-house materials evolution code REM^{2,5,7,8}. The former evaluates the neutron flux and the reaction rates in all the cells while the latter solves the Bateman equations for the evolution of the materials composition within the cells. These calculations take into account the input parameters (power released, criticality level, chemistry...), by continuously adjusting the neutron flux or the materials composition of the core. Our calculations rest on a precise description of the geometry and consider several hundreds of nuclei with their interactions and radioactive decay.

Concerning the thermal description of the reactor and the heat exchangers, the studies presented here rely on rough evaluations and aim to test the limitations of the concept. These issues will have to be studied further by specialists.

2. THE MOLTEN SALT FAST REACTOR CONCEPT

The MSFR presented here is a 3000 MWth reactor based on the Thorium fuel cycle.

2.1 Reactor geometry

As shown in Fig. 1, the core is a single cylinder (the diameter being equal to the height) where the nuclear reactions occur within the flowing fuel salt. The core is composed of three volumes: the active core the upper plenum and the lower plenum. The fuel salt considered in the simulations is a binary salt, LiF - (Heavy Nuclei)F₄, whose (HN)F₄ proportion is set at 22.5 mole % (eutectic point), corresponding to a melting temperature of 565°C. The choice of this fuel salt composition relies on many systematic studies (influence of the chemical reprocessing on the neutronic behaviour, burning capabilities, deterministic safety evaluation, deployment capabilities)^{7,8,9,10,11,12}. This salt composition leads to a fast neutron spectrum in the core.

The operating temperatures chosen for our neutronic simulations range between 700°C and 850°C, the lower limit due to the salt’s melting point, the upper limit to the structural materials chosen for our simulations and detailed below.

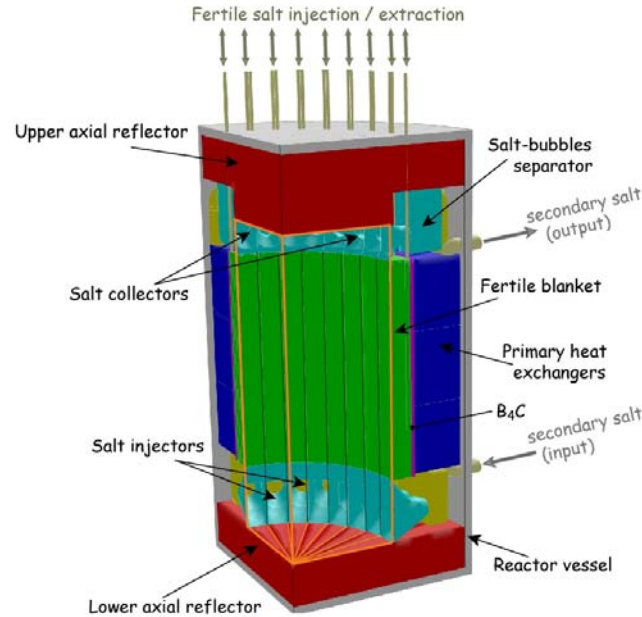


Fig. 1 Schematic view of a quarter of the MSFR, the fuel salt (not represented here) being located within the orange lines

The external core structures and the heat exchangers are protected by thick reflectors made of nickel-based alloys which have been designed to absorb more than 80% of the escaping neutron flux. These reflectors are themselves surrounded by a 10cm thick neutronic protection of B_4C which absorbs the remaining neutrons. As shown in Fig.1, the radial reflector is a fertile blanket (50 cm thick) filled with a fertile salt $LiF-ThF_4$ with 22.5%- mole ^{232}Th . Thanks to ^{233}U extraction every six months, this fertile blanket improves the global breeding ratio of the reactor.

The total fuel salt volume, one of the parameters of the present study, is distributed between the core and the external circuit (see section 2.3). This distribution impacts the fraction of delayed neutrons produced in the core and thus the safety behaviour of the core. In a rough approach, these neutrons have a quasi-uniform probability to be produced anywhere in the fuel salt, and consequently the larger the volume of salt located outside the core, the fewer the delayed neutrons produced in the core. More precise studies based on safety analyses (with seven precursor families and their decay times)⁷ have demonstrated that the reactor behaves safely with at least half of the delayed neutrons produced in the core. We have thus considered two fuel salt distributions, either 1/2 (core) – 1/2 (external circuit) or 2/3 (core) – 1/3 (external circuit).

2.2 Fuel salt reprocessing

The salt management combines a salt control unit, an online gaseous extraction system and an offline lanthanide extraction component by pyrochemistry¹³. The gaseous extraction system, where helium bubbles are injected in the core, removes all non-soluble fission products (noble metals and gaseous fission products). With the online control and adjustment of the salt composition, the reactivity can be kept equal to one. A fraction of

salt is periodically withdrawn and reprocessed offline in order to extract the lanthanides before it is sent back into the core. The actinides are sent back into the core as soon as possible in order to be burnt. The rate at which this offline salt reprocessing is done depends on the desired breeding performance. In the simulations presented here, we have fixed the reprocessing rate at 40 litres per day whatever the fuel salt volume.

2.3 Thermohydraulic considerations

The fuel salt flows upward in the core until it reaches an extraction area which leads to salt-bubble separators through salt collectors. The salt then flows downward in the primary heat exchangers and the pumps before finally re-entering the bottom of the core through injectors.

The external circuit (salt collector, salt-bubble separator, heat exchanger, pump, salt injector and pipes) is broken up in 16 identical modules distributed around the core, outside the fertile blanket and within the reactor vessel. We have divided the external circuit in two parts: the pipes (including the salt-bubble separator, the pump and the injector) and the heat exchangers. The distribution of the salt between these two parts is chosen so as to minimize the pressure drops in the circuit. The fuel salt runs through the total cycle in 3 to 6 seconds, depending on the total fuel salt volume and the salt flow velocity. The salt circulation being considered uniform, the residence time of the salt in each zone of the circuit and the core is proportional to the volume of this zone.

2.4 Physicochemical properties of the fuel salt

The initial fuel salt is composed of ${}^7\text{LiF}\text{-ThF}_4\text{-}{}^{233}\text{UF}_3$ with 77.5 mole % of LiF, this fraction being kept constant during reactor operation. The fraction of ${}^{233}\text{U}$, being adjusted to have an exactly critical reactor, depends on the total salt volume. It ranges between 2.4 mole % and 2.7 mole %. During reactor operation, fission products and new heavy nuclei are produced in the salt up to some mole % only, they do not impact the salt physicochemical properties needed for our studies. In the absence of precise data for the salt chosen in our simulations, we have used the well known characteristics of the LiF (77.5 mole%)-ThF₄ salt, presented in Table 1. The last column of Table 1 summarizes the values used in these studies, at a mean temperature of 775°C (halfway between the low and the high operating temperatures).

Table 1 Physicochemical properties used for the fuel salt

	Formula	Value at 775°C
Density ρ (g/cm ³)	$4.632 - 7.526 \cdot 10^{-4} T_{(^{\circ}\text{C})}$	4.05
Dynamic viscosity μ (Pa.s)	$0.39943 \cdot 10^{-3} \exp(2812.9/T_{(\text{K})})$	$5.85 \cdot 10^{-3}$
Thermal Conductivity λ (W/m/K)	$0.16016 + 5 \cdot 10^{-4} T_{(^{\circ}\text{C})}$	0.548
Calorific capacity c_p (J/kg/K)	-	1045

An equivalent salt (22.5 LiF-77.5 ThF₄) is used as fertile salt in the radial blanket surrounding the core and serves as radial reflector.

The secondary salt is not determined but we have assumed its characteristics to be identical to those of the fuel salt (see Table 1). In fact, the constraints on this secondary salt being less stringent than for the primary salt, its capacities in terms of heat transfers will probably be better. Our simulations thus correspond to the worst case.

2.5 Materials

The structural materials of the reactor, even if they are located around the core and not directly in it, have to bear the neutron flux together with high temperatures. We have considered for our simulations a Ni-based alloy¹⁴ containing W and Cr as detailed in Table 2.

Table 2 Composition (at%) of the Ni-based alloy¹⁴ considered for the structural materials of the core

Ni	W	Cr	Mo	Fe	Ti	C	Mn	Si	Al	B	P	S
79.432	9.976	8.014	0.736	0.632	0.295	0.294	0.257	0.252	0.052	0.033	0.023	0.004

The composition of the material used for the heat exchangers being not yet fixed, we have assumed its thermal conduction to be equal to 100 W/m/K, typical value for a metal or for graphite. This material will not be submitted to a high neutron flux; hence the choice of its composition is not too constrained.

3. OPTIMIZATION OF THE INITIAL FISSILE INVENTORY

For the earlier versions of the TMSR-NM based on a fast neutron spectrum that we studied previously^{6,8,11}, the initial fissile load was quite large, around 5 to 6 metric tons of ²³³U per GWe. This concept is reliable and robust enough to allow further optimizations, such as a minimization of the fissile inventory. The parameters for this minimization are the operating temperature of the reactor and its specific power. The operating temperature we chose is already as hot as possible for the structural materials considered here.

Thus, in this section, we will detail the impact of the specific power on the reactor's operation. With a fixed total power of 3 GWth, the specific power is modified by varying:

- The proportion of salt in/out the core. As already stated, we have considered two fuel salt distributions, either 1/2 (core) – 1/2 (external circuit) or 2/3 (core) – 1/3 (external circuit). Any value between these two limits could be chosen.
- The total fuel salt volume itself. We have considered values for the fuel salt volume ranging from 9 m³ to 30 m³. The effects of this parameter on the neutronic behaviour of the core are detailed in section 3.1.

As the MSFR uses a liquid fuel with no solid matter inside the core, the specific power can be very large compared to a reactor based on a solid fuel. The limitations are due to:

- The capacities of the heat exchangers in terms of heat extraction and the associated pressure drops (see section 3.2).
- The neutronic irradiation damages to the structural materials which modify their physicochemical properties through three effects detailed in section 3.3.

3.1 Fuel salt volume effects on the neutronics

As shown in Fig. 2 (left) for a fuel salt volume varying from 9 to 30 m³, the initial fissile inventory ranges from 1.7 to 6 metric tons of ²³³U per GWe, depending on the global conversion efficiency used*. It does not change much with the in/out of core salt distribution. Fig. 2 (right) presents the reactor's first doubling time, defined as the operating time necessary to produce in a reactor its own initial fissile inventory. The shortest doubling times, around 45 years, are obtained for a fuel salt volume ranging from 12 to 21 m³ and for only 1/3 of the fuel salt in the external circuit (red curve). Due to high neutron losses, the configurations with a fuel salt volume less than 12 m³ and half of the fuel salt out of core are not acceptable as a Generation 4 reactor, because of their poor deployment capacities.

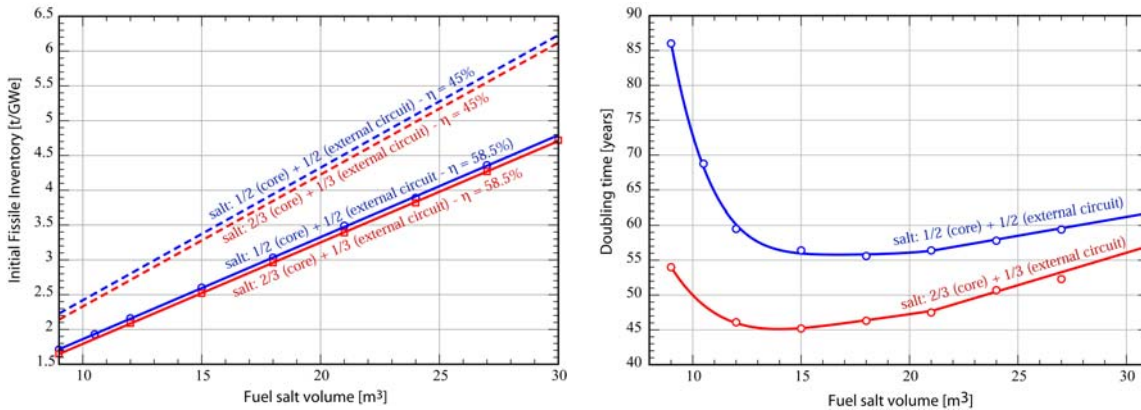


Fig. 2 Initial fissile (²³³U) inventory (left) and reactor's doubling time (right) as a function of the fuel salt volume for two in/out of core fuel salt distributions

3.2 Heat exchangers

3.2.1 Heat extraction scheme and efficiency

We have set the temperature increase during the upward flow of the salt in the core at $\Delta T = 150^\circ\text{C}$. The fuel salt is then cooled down by $\Delta T = 150^\circ\text{C}$ in the heat exchangers, the secondary salt gaining an equivalent warm-up, with a temperature difference between the

* These values are obtained while using the GWth to GWe conversion described in section 3.2.1.

primary and the secondary coolant of 150°C. We hence assumed that the mean temperature of the fuel salt ranges from 700°C to 850°C in the core, while the temperature of the secondary salt ranges from 550°C to 700°C in the heat exchangers. We may consider that the heat transfer between the secondary coolant and the third coolant (gas for example) occurs such that the output temperature of the gas is equal to 650°C for the industrial power production. With a cold source at 50°C, the Carnot yield will then be equal to $(650 - 50)/(650 + 273)$ that is 65%. We finally assume that we get 90% of this yield, i.e. a global conversion efficiency $\eta=58.5\%$. We have considered a thermal power of the core equal to 3 GWth. The extraction by Helium bubbling of the gaseous and non-soluble fission products removes around 5% of this power, i.e. 150 MWth. The electric power of the reactor is finally evaluated around $(3000 - 150)*0.585=1667$ MWe. To be very conservative, we may consider a smaller global conversion efficiency with $\eta=45\%$ only; then the final electric power is equal to around 1300 MWe. In this paper, this impacts only the initial fissile inventory per GWe as shown in Fig. 2 (left).

3.2.2 Characteristics of the heat exchangers

We have considered cross-flow plate heat exchangers, in one piece in height and vertically divided in 3 to 5 parts of $\ell=10\text{cm}$ each. The total height of these heat exchangers is equal to the height of the fertile blanket. Only 90% in height and in width are assumed to be active to take into account the structures. The thermal exchange capacity depends on the thermal conduction in the thickness “ e_s ” of the laminar layer of the salt and of the secondary coolant (see Fig. 3).

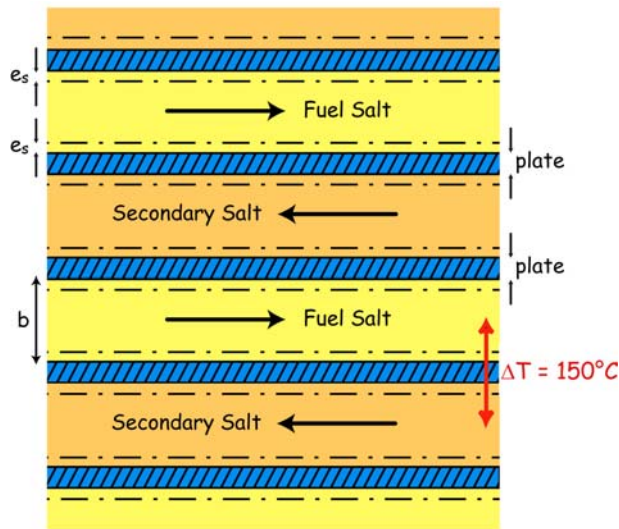


Fig. 3 Partial schematic vertical section of the plate heat exchangers, the blue striped areas representing the plates. The temperature differential of 150°C between the primary and the secondary coolants is indicated.

The interface transmission coefficient h_c may be expressed as:

$$h_c = \frac{\lambda}{e_s} = \frac{\lambda N_u}{D} \quad (1)$$

with λ the thermal conductivity of the salt (see Table 1), N_u the Nusselt number and D the diameter of the effective section of the flow. Then $e_s = D/N_u$ where:

- D is given by $D=4S/P$ where S is the real section of the flow and P its perimeter. In our case, the flow section is rectangular with a small side “b” (around some millimetres, see below) and a large side “ ℓ ” (10cm) such that $\ell \gg b$. Then $D=4b\ell/2(b+\ell) = 2b/(1+b/\ell)$.
- “b” corresponds to the gap between two plates. It is evaluated by calculating the heat transfer capacity in W/m^2 and by combining it with the volume of salt in the exchangers. The heat exchangers being designed to allow the transfer of the total power produced, this constrains the area of exchange. We finally perform a recursive calculation between the heat transfer capacity and the gap value, the results being presented in Fig. 4 for the different MSFR configurations studied here. This gap value, around 2 millimetres, does not change much with the in/out of core salt distribution.

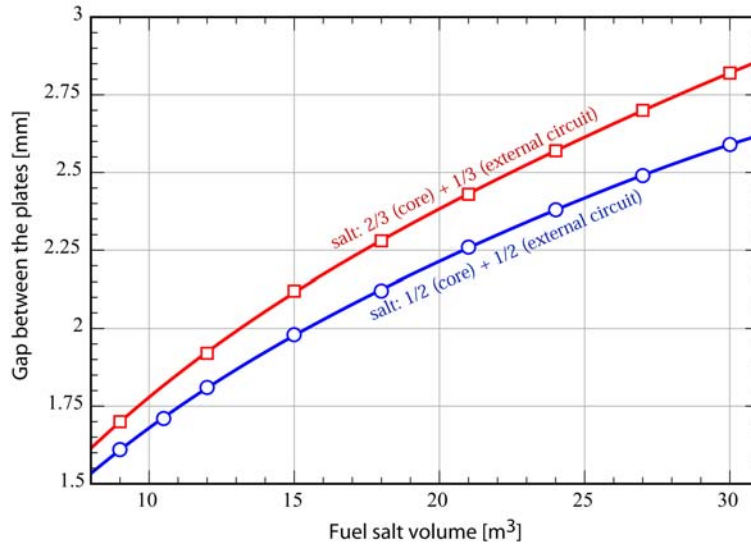


Fig. 4 Values of the gap between the plates of the heat exchangers as a function of the fuel salt volume for two in/out of core distributions of the fuel salt

- The Nusselt number is given by¹⁵:

$$N_u = 0.0296 \text{ Re}^{0.8} \text{ Pr}^{0.43} \quad (2)$$

- The Prandtl number Pr is equal to $c_p \mu / \lambda$ with c_p the calorific capacity of the salt and μ its dynamic viscosity (see Table 1).

- The Reynolds number “Re” is defined as $\rho V D / \mu$ where ρ corresponds to the salt’s density (see Table 1) and V its velocity. The velocity of the salt in the heat exchangers is calculated as the height of the exchangers divided by the residence time of the salt in the exchangers.

3.2.3 Pressure drop in the external circuit

The pressure drops in the core itself, equal to around 10^{-4} bar, are negligible and will not be considered in the following.

The pressure drop in a pipe is given by $\frac{1}{2} L \lambda \rho V^2 / D$. L is the pipe’s length and λ a pressure drop coefficient calculated through the Colebrook equation approximated by Haaland for the turbulent case as $\lambda^{-1/2} = -1.8 * \text{Log}_{10} [6.9 / \text{Re} + (\epsilon / 3.7 D)^{1.11}]$. We have considered a value of 10^{-5} m for the roughness of the pipe surface “ ϵ ”. We have also added the singular pressure drops in the pipes due to the bends, equal to $\frac{1}{2} \kappa \rho V^2$ per bend where κ is the pressure drop module equal to 0.6 for a bend of 90° .

The total pressure drop is finally translated in terms of pump capacities through the evaluation of the electrical power to be delivered to each pump as detailed in Eq. (3) where we assumed a pump efficiency of 60%.

$$P \text{ [kW]} = (\text{Flow per pump [m}^3/\text{s]}) * (\text{Pressure drop [Pa]}) / (\text{Pump efficiency}) \quad (3)$$

The results are presented in Fig. 5. It appears that the MSFR configurations with only 1/3 of the fuel salt in the external circuit and which contain less than 15 m^3 may be unacceptable if we assume that requiring more than 300 kW to operate a pump is unrealistic¹⁶.

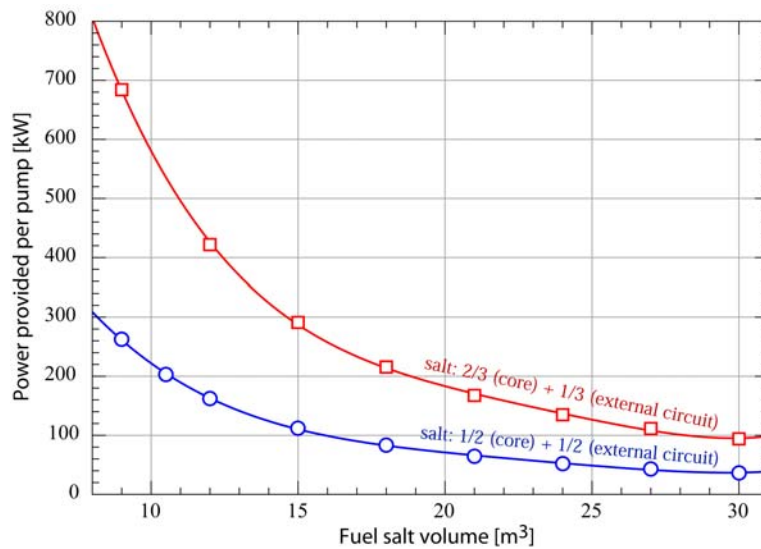


Fig. 5 Pump capacities as a function of the fuel salt volume for two in/out of core fuel salt distributions

3.2.4 Summary

In spite of the simplified considerations we used in this section for the thermal evaluation of the heat exchangers, some tendencies concerning the MSFR configurations clearly come out. The best compromise between the deployment capacities (Fig. 2 right) and the pump power (Fig. 5) corresponds to the medium fuel salt volumes. Concerning the fuel salt distribution in the system, the deployment capacity criterion favours the configurations with only 1/3 of the fuel salt out of the core, while the pump capacity criterion favours the configurations with half of the fuel salt out of the core. In the following, to be conservative, we will give precedence to the technological limitations and thus present the results of the materials considerations for the MSFR configurations with half of the fuel salt out of the core.

3.3 Materials considerations

The neutronic irradiation damages to the structural materials modify their physicochemical properties through three effects: the displacements per atom, the production of Helium gas via nuclear reactions in the materials, and finally the transmutation of the Tungsten (component of the Ni-based alloy selected for this study) to Osmium through nuclear reactions. We have calculated these damages for the axial reflectors, which are the most irradiated elements of the core. For improved legibility, precise results will be given only for the medium case corresponding to a fuel salt volume of 18 m³.

3.3.1 Displacements per atom

The radiation damages in neutron-irradiated materials, dependent on many factors like the irradiation dose and the neutron spectrum, are expressed in dpa (displacements per atom), corresponding to the number of times an atom is displaced for a given fluence. Our calculations show that the damages are largest in the first two centimeters of the central area (radius 20 cm and thickness 2 cm) of the axial reflector and are quite small, only 1.17 dpa /year with a fuel salt volume of 12 m³ to 0.47 dpa /year with 27 m³. Thus, this is not a limiting factor for our present studies. We did not consider here the dpa due to the fissions occurring near the materials which damage them on the first few ten micrometers only.

3.3.2 Helium Production

The Helium concentration in the structural materials is directly determined by its production rates through nuclear reactions. This He production depends on the boron and nickel contents of the alloy used as structural material, He appearing through the two reactions: $^{10}\text{B}(n, \alpha)^7\text{Li}$ and $^{58}\text{Ni}(n, \alpha)^{55}\text{Fe}$. As shown in Fig.6 and contrary to the case of thermal reactors, the reaction involving ^{58}Ni is dominant here. Moreover the boron content of the alloy may be easily reduced, the values indicated here being a maximum. The largest acceptable amount of Helium in the alloy is not presently known: the diffusion of Helium at the temperatures involved in the system has not been studied.

We assumed that the acceptable limit is equal to 100 ppm of He and that there was no He leak by diffusion. The results are displayed in Fig. 7 for a fuel salt volume of 18 m^3 in terms of reactor operation times necessary to produce this amount of 100 ppm of He in different depths of the axial reflector. This operation time for deeper zones of the reflector being equal to more than 170 years (for 14 cm to 30 cm) is not indicated in the figure. As a conclusion, regular replacements of the most irradiated area of the upper axial reflector will have to be planned, but this concerns only its first 15 centimeters.

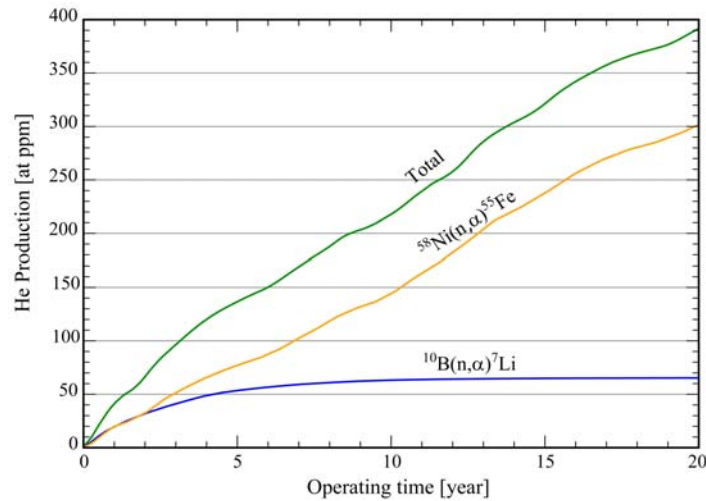


Fig. 6 Contributions of the different nuclear reactions involved in Helium production in the most irradiated part of the axial reflector (radius 20 cm and thickness 2 cm), as a function of the reactor operating time, for a fuel salt volume of 18 m^3

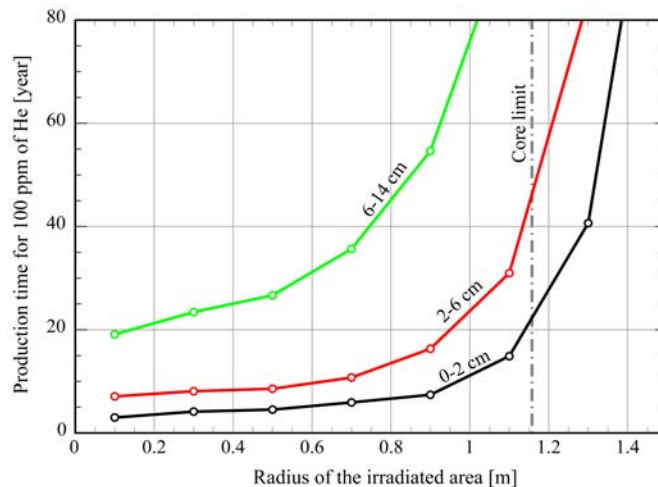


Fig. 7 Operation time necessary to produce 100 ppm of He in different depths of the axial reflector, as a function of the irradiated area considered (zero corresponding to the centre of the core), with a fuel salt volume of 18 m^3

3.3.3 Osmium Production

During our neutronic simulations, we noticed the transmutation of the Tungsten contained in the alloy into Rhenium and Osmium through nuclear reactions as detailed in Fig. 8. The consequences of this effect on the materials resistance are to be investigated; if a loss of less than 1 at% of tungsten is acceptable, then the most irradiated part of the upper reflector will have to be changed every 5 to 10 years as shown in Fig. 9. This part will anyway be regularly replaced because of its Helium content (see section 3.3.2).

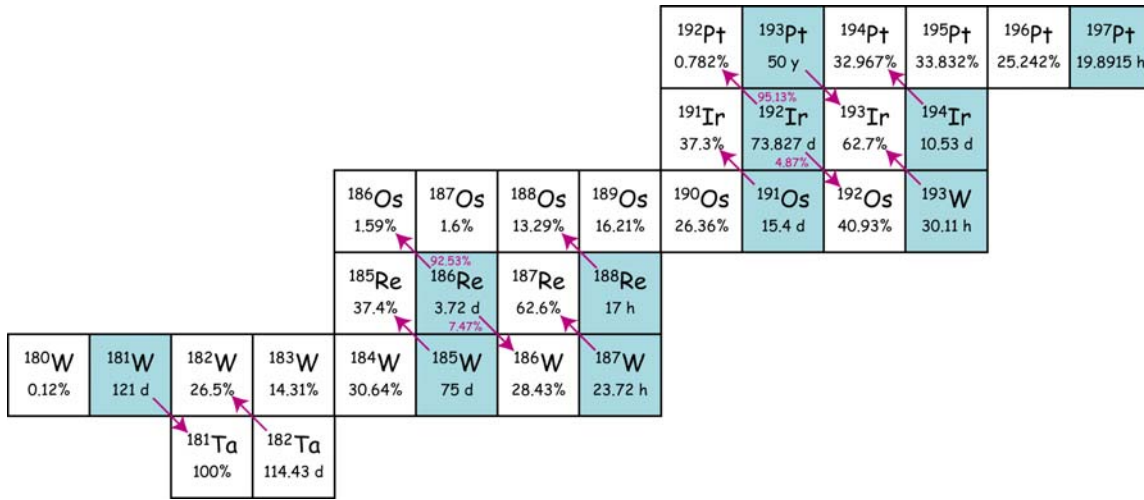


Fig. 8 Transmutation cycle of Tungsten, Rhenium and Osmium, due to the neutronic captures; the blue boxes represent the unstable nuclei that decay through the purple arrows

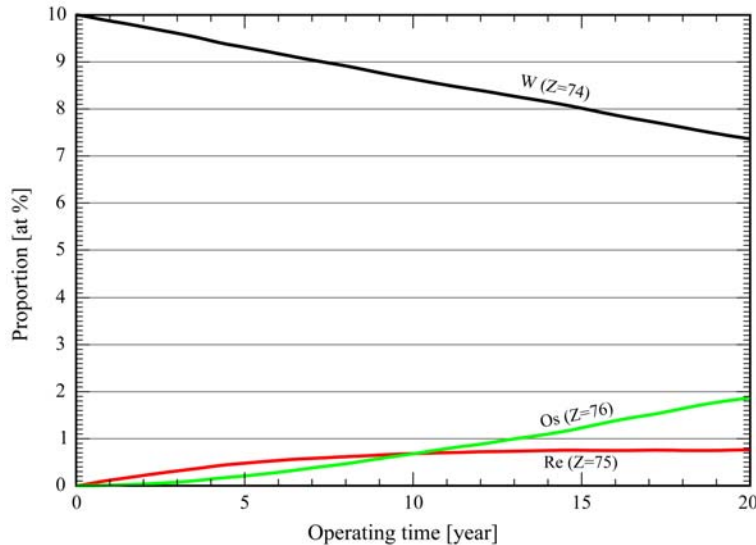


Fig. 9 Contents in Tungsten (W), Rhenium (Re) and Osmium (Os) of the most irradiated part of the axial upper reflector (central area of radius 20 cm and thickness 2 cm), with a fuel salt volume of 18 m³

3.3.4 Summary

We present in Table 3 the results obtained for the different irradiation damages as a function of the fuel salt volume, in terms of reactor operation times necessary to produce these damages. We notice that the damages are inversely proportional to the fuel salt volume of the reactor, thus logically favoring the larger MSFR configurations. To conclude and with the hypotheses taken here in terms of damage limitations, the most constraining effect seems to be the Helium production in the structural materials but this has to be thoroughly studied by specialists.

Table 3 Reactor operation time necessary to produce 100 dpa (second column), 100 ppm of He (third column) and the loss of 1 at% of Tungsten (fourth column) in the most irradiated part of the axial reflector (central area of radius 20 cm and thickness 2 cm), for different fuel salt volumes of the MSFR

Fuel salt volume	t(100 dpa)	t(100 ppm He)	t(-1 at% of W)
12 m ³	85 years	2.2 years	4.7 years
18 m ³	133 years	3.2 years	7.3 years
27 m ³	211 years	5.5 years	10.9 years

CONCLUSIONS

The Molten Salt Fast Reactor (MSFR) concept is particularly well suited to fulfill all the criteria defined by the Generation IV International Forum (GIF) and has been selected for further studies by the GIF. This concept is reliable and robust enough to allow further optimizations, such as the minimization of the fissile inventory presented here. More precisely, we have evaluated the impact of the specific power on the reactor's operation, by varying the total fuel salt volume and the fuel salt distribution in the system (in/out the core). These optimization studies, although relying on rough evaluations for the thermal description of the heat exchangers, are sufficient to test the limitations of the concept in terms of materials damage and heat evacuation efficiency and to bring to light the following general tendencies.

Regarding the neutronic considerations, the reactor doubling time and thus the deployment capacities are optimized for a fuel salt volume ranging from 12 to 20 m³, favouring the reactor configurations with only 1/3 of the fuel salt out of the core.

The MSFR configurations with the smaller fuel salt volumes, which produce the largest pressure drops in the external circuit, require pumps with better performances. Consequently the reactor configurations with a larger part of the fuel salt out of the core (limited to half of the fuel salt in the present studies for safety considerations) are here preferable.

Finally the irradiation damages are inversely proportional to the fuel salt volume of the reactor, thus logically favoring the larger MSFR configurations. These damages are dominated by Helium production through the (n, α) reaction on ⁵⁸Ni. Two solutions

may be considered: either regularly replacing the superficial layers (around 15 cm) of the axial reflectors and the fertile blanket container; or selecting another material without boron or ^{58}Ni . The latter solution may prove more expensive but will be reserved to the more exposed areas. The effects of Helium on the structural materials (maximal acceptable amount, diffusion) have to be thoroughly studied by specialists to confirm our preliminary conclusions. Likewise, the effects of the transmutation to Osmium of the Tungsten contained in the structural materials have to be studied for a better understanding of the long-term materials resistance.

Our studies demonstrate that an initial ^{233}U inventory lower than 4 metric tons per GWe may be reached even with the limitations assumed for the irradiation damages to the structural materials. If more thorough studies show that our assumptions on materials behavior under irradiation are pessimistic and that the limits can be pushed further, a fissile inventory lower than 2.5 tons per GWe may be reached. Realistic evaluations of the overall possibilities of the MSFR strongly depend on further research in the fields of materials and heat exchangers.

ACKNOWLEDGMENTS

The authors wish to thank PACEN (Programme Aval du Cycle Electronucleaire) of the *Centre National de la Recherche Scientifique* (CNRS) for its support. We are also very thankful to Elisabeth Huffer for her help during the translation of this paper.

REFERENCES

1. M.E. WHATLEY et al., "Engineering development of the MSBR fuel recycle", *Nuclear Applications and Technology*, **8**, 170-178 (1970)
2. L. MATHIEU, "Cycle Thorium et Réacteurs à Sel Fondu : Exploration du champ des Paramètres et des Contraintes définissant le Thorium Molten Salt Reactor", PhD-thesis, Institut National Polytechnique de Grenoble, France (2005)
3. L. MATHIEU, D. HEUER et al, "Proposition for a Very Simple Thorium Molten Salt Reactor", *Proceedings of the Global international conference*, Tsukuba, Japan (2005)
4. L. MATHIEU, D. HEUER et al, "The Thorium Molten Salt Reactor: Moving on from the MSBR", *Prog in Nucl En*, **48**, 664-679 (2006)
5. A. NUTTIN, D. HEUER et al, "Potential of Thorium Molten Salt Reactors", *Prog. in Nucl. En.*, **46**, 77-99 (2005)
6. E. MERLE-LUCOTTE, "Le cycle Thorium en réacteurs à sels fondus peut-il être une solution au problème énergétique du XXI^{ème} siècle ? Le concept de TMSR-NM", *Habilitation à Diriger les Recherches, Institut Polytechnique de Grenoble*, France (2008)

7. C.W. FORSBERG, C. RENAULT, C. LE BRUN, E. MERLE-LUCOTTE, V. IGNATIEV, “Liquid Salt Applications and Molten Salt Reactors”, *Revue Générale du Nucléaire* N° 4/2007, **63** (2007)
8. E. MERLE-LUCOTTE, D. HEUER et al., “Optimization and simplification of the concept of non-moderated Thorium Molten Salt Reactor”, *Proceedings of the International Conference on the Physics of Reactors PHYSOR 2008*, Interlaken, Switzerland (2008)
9. J.F. BRIESMEISTER, “MCNP4B-A General Monte Carlo N Particle Transport Code”, Los Alamos Lab. report LA-12625-M (1997)
10. E. MERLE-LUCOTTE, L. MATHIEU, D. HEUER, V. GHETTA et al., “Influence of the Processing and Salt Composition on the Thorium Molten Salt Reactor”, *Nuclear Technology*, **163**, Number 3, 358-365 (2008)
11. E. MERLE-LUCOTTE, D. HEUER, M. ALLIBERT, V. GHETTA, C. LE BRUN, “Introduction of the Physics of Molten Salt Reactor”, *Materials Issues for Generation IV Systems, NATO Science for Peace and Security Series - B, Editions Springer*, 501-521 (2008)
12. E. MERLE-LUCOTTE, D. HEUER, C. LE BRUN and J.M. LOISEAUX, “Scenarios for a Worldwide Deployment of Nuclear Power”, *International Journal of Nuclear Governance, Economy and Ecology*, **1**, Issue 2, 168-192 (2006)
13. S. DELPECH, E. MERLE-LUCOTTE, D. HEUER, M. ALLIBERT, V. GHETTA, C. LE BRUN, L. MATHIEU, G. PICARD, “Reactor physics and reprocessing scheme for innovative molten salt reactor system”, *J. of Fluorine Chemistry*, **130**, Issue 1, 11-17 (2009)
14. R.CURY, “Etude métallurgique des alliages Ni-W et Ni-W-Cr : relation entre ordre à courte distance et durcissement”, PhD-Thesis, Université Paris XII, France (2007)
15. J.H. Lienhard IV and J.H. Lienhard V, “A Heat Transfer Textbook”, *Phlogiston Press, Cambridge Massachusetts*, 325 (2008)
16. E. VENTRE, “Réacteurs à sels combustible fondu – Conception d’un bloc pile à circuit primaire intégré”, *EDF Direction des Etudes et Recherches, internal note T10/SELST21/600, C9* (1976)